

Progressive Morphology Development to Produce Multilayer Films and Interpenetrating Blends by Chaotic Mixing

O. KWON, D. A. ZUMBRUNNEN

Center for Advanced Engineering Fibers and Films and the Department of Mechanical Engineering, Clemson University, Clemson, South Carolina 29634-0921

Received 16 November 2000; accepted 9 December 2000

ABSTRACT: Chaotic mixing of immiscible binary components was recently used in a continuous flow process to obtain extruded films with very many internal layers. Where interfacial tension is small, individual layer thicknesses can be only tens of nanometers and many thousands of continuous or broken layers can be formed. Such materials are both novel and potentially important. In this study, multilayer film formation and breakup were investigated systematically by using a batch chaotic mixer to better understand the more industrially relevant continuous flow counterpart. Polystyrene (PS) and low-density polyethylene (LDPE) were used as a model binary system with appreciable interfacial tension such that comparatively thicker layers and larger breakup bodies were formed and more readily examined. The multilayer film morphology developed progressively as chaotic mixing continued and was thereby amenable to control and optimization with regard to layer thickness and number. Blends with single or dual phase continuity and structured droplet distributions were found to be important derivative morphologies upon layer breakup. © 2001 John Wiley & Sons, Inc. *J Appl Polym Sci* 82: 1569–1579, 2001

Key words: chaotic mixing; films; interpenetrating blends; coextrusion; permeation; membranes

INTRODUCTION

Polymer film products often consist of more than one layer, where each layer imparts a particular functionality such as permeation resistance to water or oxygen, and mechanical strength. Fewer than six layers are most often used to balance performance with manufacturing complexity.¹ However, it is often more preferable to have large

numbers of thin layers in lieu of fewer thick layers because material performance is better maintained upon deformation and improved flexure is obtained. Layer multiplication devices were developed as a result to give extruded films consisting of up to several thousand layers. Multilayer films have improved impact strengths and fatigue resistances owing to improved ductility of thin layers and increased resistance to crack propagation.^{2,3} Light interactive films such as polarizers and refractive media can also be produced where many internal layers can be formed. Experimental evidence suggests that permeation may decrease as the number of film layers is increased for a fixed composition.⁴ Processes for producing multilayer films are thereby of significant importance.

Correspondence to: D. A. Zunbrunnen (zdavid@ces.clemson.edu).

Contract grant sponsor: Engineering Research Center Program of the National Science Foundation; Contract grant number: EEC-9731680; Contract grant sponsor: 3M Company.

Journal of Applied Polymer Science, Vol. 82, 1569–1579 (2001)
© 2001 John Wiley & Sons, Inc.

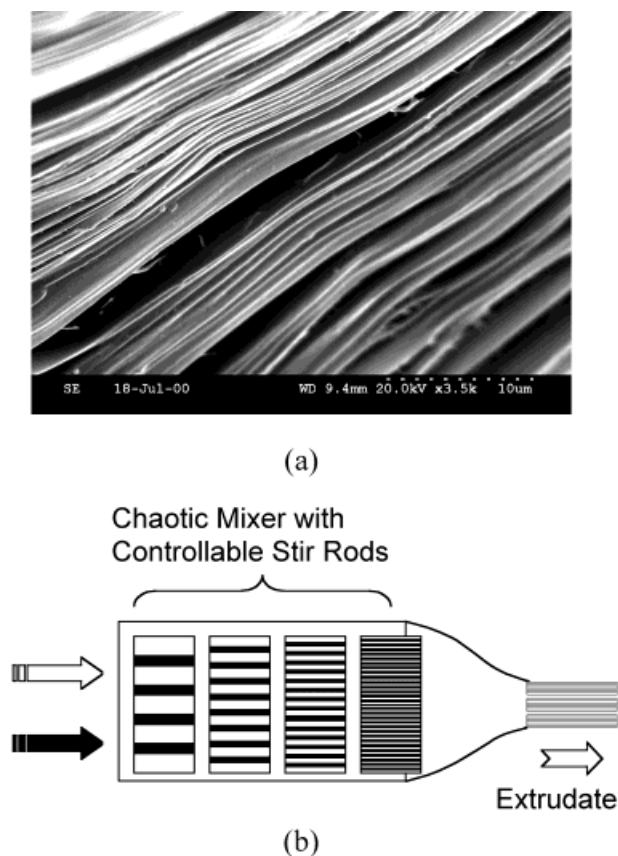


Figure 1 (a) Highly multilayered film morphology in an extruded 2.5-mm monofilament composed of 20% by volume EPDM and PP. (b) Conversion by recursive stretching and folding of two polymer melt streams to a blend with distributed multilayer films and subsequent extrusion.

Two thermoplastics were recently combined in the melt by a new practical process to obtain extruded films and fibers with thousands of unbroken internal layers.⁵ A multilayer morphology is shown in Figure 1(a) for a blend consisting of 20% by volume ethylene-propylene-diene terpolymer (EPDM) and polypropylene (PP). Individual film layers were formed *in situ* by chaotic mixing and subsequently extruded through a linear taper die in the form of a 2.5-mm filament. The layer thicknesses were less than 200 nm and numbered in the many thousands. Individual layers were separated by fracturing samples after soaking in liquid nitrogen. However, layers with smaller thicknesses (<100 nm) were also produced that did not separate upon fracture, perhaps due to morphology changes or elevated toughness of the ultrathin layers. Layer thicknesses and the number of layers were also selectable. The particular

chaotic mixer that was used consisted of a fixed cylindrical barrel and two internal stir rods that were alternately and periodically rotated by an automated drive system. The highly multilayered extrudate was thereby obtained from a device having less complexity and greater operational flexibility (e.g., on-line control of internal layer thickness, number of layers, and derivative morphologies) than alternate technologies for producing films with even fewer numbers of layers. The actual amount of layer refinement that was possible depended on the particular polymer combination.

Chaotic mixing can be instilled within mixing devices by the motions of bounding surfaces, such as stir rods or barrels. Consequently, polymer melts undergo laminar shear deformations that are known to decrease thicknesses of component bodies. For laminar shear alone, an initially rectangular minor component of width w is reduced after a total strain γ by a factor $[1 + \gamma^2]^{-1/2}$.⁶ However, in concert with refinement due to laminar shear, regions within melts are also folded over time such that the number of layers is increased. Folding causes the envelopment of previously segregated melt such that compositional uniformity improves over time at smaller length scales. Stretching and folding in this manner creates horseshoe mappings that are characteristic of chaotic systems. This situation is depicted in Figure 1(b), where the dark band denotes a minor component melt stream and the white region denotes the surrounding major component melt stream. Both melt streams are stretched and folded recursively about one another until a blend emerges with a multilayer morphology that may be extruded. The blend morphology is thereby developed progressively and layer thicknesses decrease over time. The thickness δ of minor component layers relative to the initial combined thickness σ_0 for one initial major and minor component layer is related by volume conservation to the n number of folding operations by $\delta/\sigma_0 = \phi/2^n$, where ϕ is the volume fraction of the minor component. Combining this expression and the one above for shear-induced deformation, potential film-layer refinement by chaotic mixing can be expressed by eq. (1). In practice, however, shear rates are not spatially uniform and folding can occur with differing periodicities within chaotic mixing devices so that films of different thicknesses arise. Interfacial effects also slow chaotic mixing and lead to film breakup after a certain level of refinement is attained.⁷ Equation (1) is

useful for determining the maximal amount of reduction in layer thickness that can be achieved. For $\sigma_0 = 1$ cm and $\varphi = 0.5$, for example, layer thicknesses of less than 100 nm would be obtained for $n > 15$ and $\gamma > 0$:

$$\frac{\delta}{\sigma_0} = \frac{\phi}{2^n} \left(\frac{1}{\sqrt{1 + \gamma^2}} \right) \quad (1)$$

Although the highly multilayered blend of Figure 1(a) is itself useful, the layers can also serve as a parent morphology to other useful blend morphologies. Layer instabilities in melts processed by chaotic mixing and consisting of low-density polyethylene (LDPE) and poly(ethylene-stat-vinyl acetate) or polystyrene (PS) at low minor component concentrations were documented in which long parallel ridges formed.^{8,9} The ridge troughs deepened until layers fragmented into fibers in a manner analogous to capillary instabilities. Having been derived from parallel tears in thin layers, the fibers had high aspect ratios and diameters similar to the layer thicknesses. Computational modeling and the examination of specimens suggested that the instabilities were promoted by folding of the films, as especially occurs during three-dimensional chaotic mixing.⁷ Multilayer blend morphologies can thereby serve as a pathway to also form fiber-reinforced blends. Additional derivative blend morphologies may be disclosed by further investigations of how layers of this type break up in the melt.

It is commonly misunderstood that processes based on chaotic behavior are uncontrollable. It is true that the physical locations of particular blend features within a chaotic mixing device are sensitive to even minute process variations. However, overall blend morphologies are consistently reproducible and their development can be controlled by simply adjusting process duration or parameters related to chaotic mixing.¹⁰ In contrast, common blending equipment such as most types of extruders and batch mixers were designed to achieve a well-mixed state by breaking down any initial or evolving structures among components such as sheets, films, or fibers. In effect, structure among polymer components and additives in these devices is often first degenerated and later reconstructed in extrusion steps where comparatively less opportunity exists for influencing blend morphology due to much smaller melt residence times in dies than in the mixing devices themselves.

Because the direct production of multilayer films by coextrusion involves increased complexity, process engineers often employ screw extruders to create blends where the minor component becomes elongated within the melt into small filmlike pieces after passing through film dies.^{11,12,13} In this manner, the properties of multilayer films can be approached. Much time can be consumed identifying narrow operational windows and making equipment alterations. These processes generally require that abundant droplets be formed of sufficiently high capillary number so that stretching can occur either in the extruder itself or in the die. In contrast, the process shown in Figure 1(b) promotes the direct and progressive formation of film layers and important derivative blend morphologies.

In this study, multilayer film formation by chaotic mixing was investigated systematically by batch processing to elucidate how multilayers form *in situ* and eventually break up in a companion industrially relevant process (Fig. 1). Subsequent important morphologies that can be obtained after different extents of layer breakup were also identified. These included blends with single- and dual-phase continuity and structured droplet distributions. PS as the major component and LDPE were used as a model binary system with appreciable interfacial tension such that comparatively thicker layers than those in Figure 1 and larger breakup bodies were formed to facilitate morphology inspections.

EXPERIMENTAL

Multilayer film formation was investigated systematically by using a batch chaotic mixer to better understand the more industrially relevant continuous flow counterpart depicted in Figure 1(b). In Figure 1(b), chaotic mixing occurred within vertical planes so that locally parallel multilayer films arose [Figure 1(a)], refined progressively, and were transported downstream toward a die. The batch chaotic mixer in Figure 2 provided a similar chaotic mixing condition and was therefore selected for this study. The mixer was installed in an electric oven so that thermoplastic contents could be processed in the melt state at a specified temperature. Chaotic mixing occurred in the space between an inner cylinder and an outer cylinder of radii r_{in} and r_{out} , respectively. The outer cylinder was made from a Pyrex glass tube with $r_{out} = 23.5$ mm. The inner cylinder was stain-

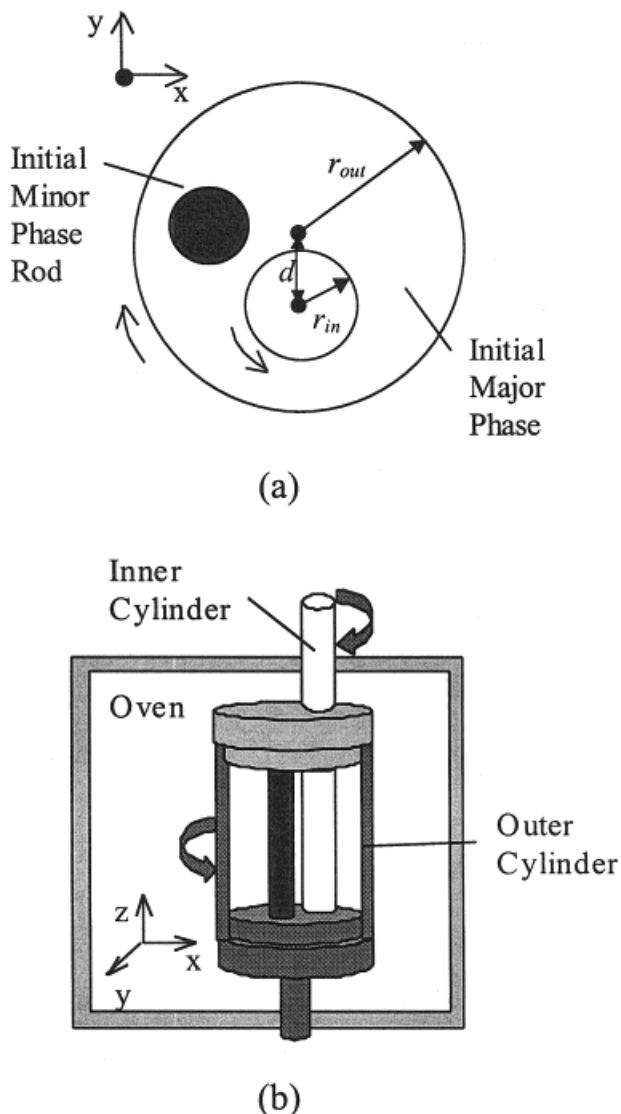


Figure 2 (a) Cross section of the two-dimensional chaotic mixer and the initial location of minor phase in rod form. (b) Schematic representation of mixer installed in oven.

less steel with $r_{in} = 7.5$ mm. The inner cylinder axis was offset by a distance $d = 8.6$ mm from the outer cylinder axis. A 12-cm cavity height was used to mitigate end effects and promote two-dimensional flow fields and thereby the formation of parallel film layers over central portions of the cavity.

Chaotic mixing was induced by alternately and repetitively rotating the inner and outer cylinders by using an automated drive system. Details of the drive system were reported previously.¹⁴ The radius ratio $\xi (= r_{out}/r_{in})$, the distance between the cylinder axes given by a parameter $\epsilon [= d/(r_{out}$

$- r_{in})]$, and the rotational displacements must be selected to give chaotic mixing conditions throughout the cavity.^{15,16} In this study, $\xi = 3.13$ and $\epsilon = 0.54$. The angular rotations for the inner and outer cylinders were specified to give equal linear displacements so that both cylinders induced similar kinematical changes. The inner cylinder was thereby rotated 3.8 rotations and the outer cylinder was rotated 1.2 rotations. Rotational displacements were done according to a mixing protocol, and the extent of mixing was controlled by the N number of mixing periods, where one period consisted of one set of cylinder motions. In the periodic protocol, the inner and outer cylinders were separately and sequentially rotated in opposite directions. For $N = 3$, for example, the periodic protocol can be described in terms of rotational motions for the inner (I) cylinder and outer (O) cylinder as follows: $O-I-O-I-O-I$. An aperiodic mixing protocol was shown to promote more uniform stretching¹⁷ and thereby blends with more uniform morphologies.⁹ With this protocol for $N = 1$, the outer cylinder was first rotated and stopped, and the inner cylinder was subsequently rotated and stopped (i.e., $O-I$). The complement of this sequence was appended to determine the motion ($I-O$) for $N = 2$. Similarly, the complement of the entire prior motion ($O-I-I-O$) determined the motion ($I-O-O-I$) for $N = 3$ and 4, and so forth. In this study, the periodic mixing protocol was used for $0 \leq N \leq 8$ to assess early morphology development in response to simpler periodic motions of the inner and outer cylinders. The aperiodic mixing protocol was used for larger N for which compositional uniformity was also desirable.

PS and LDPE were used as a model binary system with appreciable interfacial tension such that comparatively thicker layers than those in Figure 1(a) and larger breakup bodies were formed and more readily examined. Atactic PS (Nova Chemicals Inc., GPPS 555, Calgary, Alberta, Canada) was employed as the major component and LDPE (Eastman Chemical Products, Inc., 18BOA, Kingsport, TN) served as the minor component. The shear rates corresponding to the angular speeds of the inner and outer cylinders (< 2 rpm) ranged from 0.09 to 0.21/s and from 0.03 to 0.57/s, respectively. Viscosities were measured with cone and plate viscometer (Rheometric Scientific, RMS 800, Piscataway, NJ) in the low-shear-rate range at two different temperatures and are presented in Figure 3. The viscosity ratio (LDPE/PS) varied from 0.05 to 0.07 for the shear

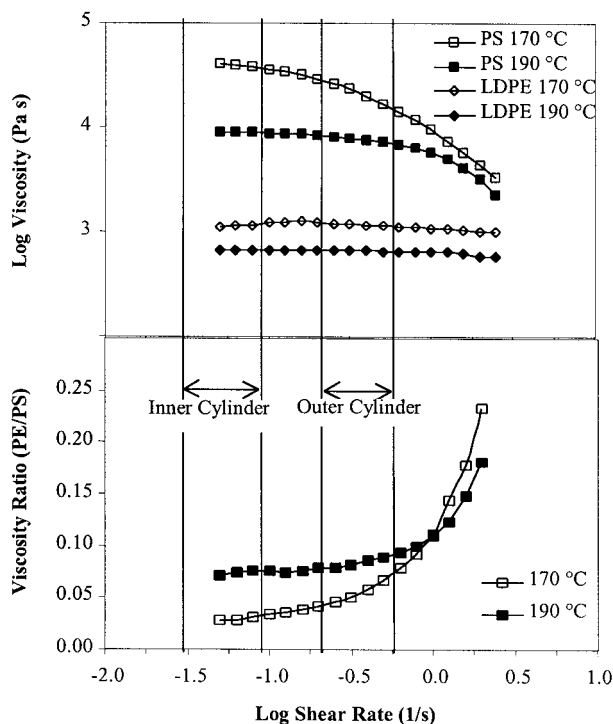


Figure 3 Viscosity and viscosity ratio for PS and LDPE.

rates above. This low value is associated with early breakup because interfacially driven flows within minor component bodies can become more quickly organized to yield high-magnitude interface instabilities.^{7,18,19} Surface tension values of LDPE and PS were adapted from the work by Sanchez.²⁰ The corresponding interfacial tension between LDPE and PS was determined to be 4.5 dyn/cm.²¹ The transition temperatures were measured with a differential scanning calorimeter (TA Instruments, New Castle, DE) at a heating rate of 10°C/min. The glass transition temperature of PS was determined to be 81°C and the melting temperature of LDPE was 114°C.

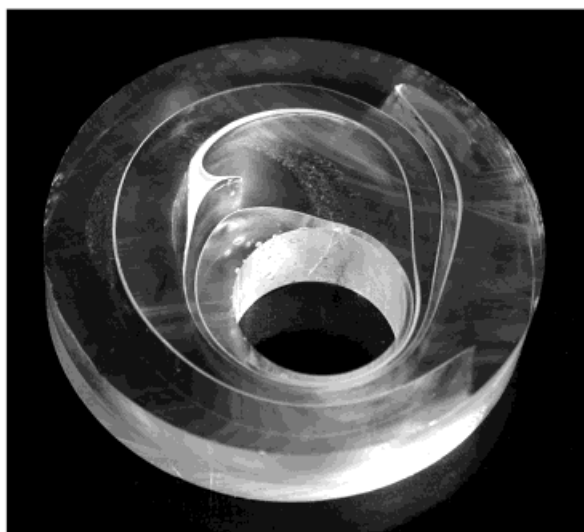
Separate specimens were produced after chaotic mixing was continued for a specified number of mixing periods. Identical initial configurations of the minor and major phases were used for each polymer combination so that morphology differences were due only to differences in processing times. This initial configuration is shown in Figure 2 and consisted of the minor component in rod form within the major component. The LDPE minor phase was initially a rod of 11.1 mm diameter and 12 cm height. The corresponding overall volume fraction was 6.4%. To arrange this initial configuration, void-free castings of PS were first

formed directly within the outer cylinder. A vertical hole was drilled in the casting and injected with LDPE melt. A separate hole was drilled in the PS casting to accommodate the inner cylinder of the mixing cavity. After the prescribed number of mixing periods was completed, the cavity and its contents were quickly placed into a reservoir of ice water. A plunger was pressed onto the upper melt surface to suppress void formation due to thermal contraction. Samples were cooled to below the glass transition temperature of PS within 10 min.

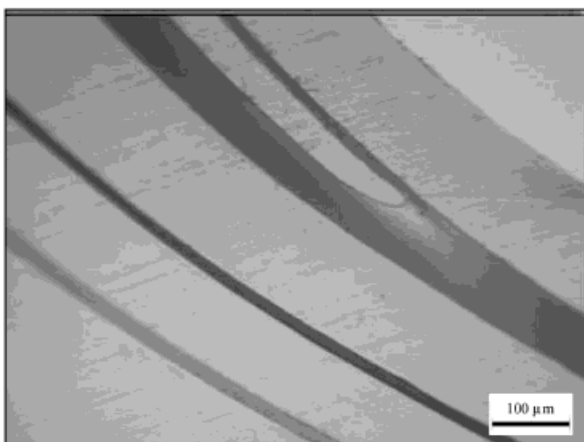
For the structural examination of the blends, specimens were obtained from the central 6-cm portion of the entire cylindrical samples where end effects were smallest and mixing was predominately two-dimensional. For optical microscopy, 300- μm -thick slices were cut along planes oriented perpendicular to the rod axes with a diamond linear precision cutter. The slices were polished with a silk lap and 0.05 μm alumina powder in water. For short mixing times and larger blend feature sizes, optical micrographs were captured by a frame grabber with a 640 \times 480 pixel resolution. LDPE film-layer thicknesses or sizes of other structures were measured at 100 different locations. The smallest and largest dimensions were recorded and the average dimensions were calculated from the 100 individual measurements. For blends produced for longer mixing times and containing thinner films, specimens were fractured after immersion in liquid nitrogen for 5 min. Examinations of fracture surfaces were done by low-voltage field emission scanning electron microscopy (Hitachi Model 4700, Tokyo, Japan) in orientations parallel and perpendicular to the cylinder axes of the mixing cavity. This mode of SEM allowed morphology inspections without gold sputtering. Three-dimensional views of more complex morphologies were also obtained by dissolution of the PS matrix with toluene at room temperature and collection of liberated LDPE structures on filter paper.

RESULTS AND DISCUSSION

Multilayer film formation and breakup were investigated systematically by producing samples for increasing mixing times, where the mixing time was given in terms of the number N of chaotic mixing periods described above. The multilayer film morphology developed progressively as chaotic mixing continued and was thereby ame-



(a)



(b)

Figure 4 (a) A 2-cm-thick casting containing a continuous single LDPE film formed after one mixing period ($N = 1$) in a PS matrix. (b) Magnified view of the region close to the inner cylinder in the narrow gap between the two cylinders of the mixing cavity.

nable to control and optimization with regard to layer thickness and number of layers, and also the extent of layer breakup. This feature suggested a basis for the development of more controllable blending processes as well as processes where unique morphologies can be formed. Early film formation ($N = 1$) is shown in Figure 4(a). The single initial LDPE rod of Figure 2 was converted into a continuous film with three folds and four ends. The film in Figure 4(a) was uniform over an 8 cm height where two-dimensional chaotic mixing was not affected by proximity to the

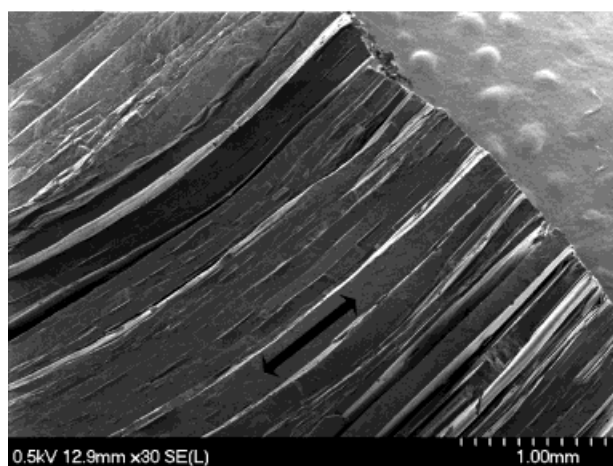
upper and lower cavity surfaces. The central 6-cm portions were used for morphology examinations. The film thickness ranged along the film length from $6 \mu\text{m}$ at the film ends to $30\text{--}200 \mu\text{m}$ in the middle regions, excluding an irregularly shaped body in the 10 o'clock position. Significantly, the initial LDPE rod was reduced in thickness on average by two orders of magnitude after only one mixing period without breaking. This refinement rate is consistent with eq. (1).

Close inspection of the film in Figure 4(a) revealed the presence of folds and multiple film layers. Although only one mixing period elapsed that consisted of the sequential rotation of the inner and outer cylinders in Figure 2, three folds were generated. Two folds were evident at the 10 o'clock and 1 o'clock positions. One fold with a small curvature and several thin parallel films are shown in a magnified view in Figure 4(b). The folds are important features. In Figure 4(a), for example, thin films at the 10 o'clock position converge on a large LDPE domain. PS began infiltrating the LDPE domain in a nascent fold. A portion of the LDPE domain will thereby be converted into a film layer by stretching instilled by subsequent cylinder motion. Folding caused the envelopment of previously segregated melt such that compositional uniformity improved over time at smaller length scales. Similar morphological changes occurred in the PS major component; the leading edge of the short film in Figure 4(a) at the 10 o'clock position can be regarded as the interior of a fold in PS. With this perspective, it can be understood that stretching and folding caused the mutual envelopment of one component by the other. This characteristic is distinctly different from what occurs in simple flows. However, it should be noted that a range in film thicknesses were produced. In Figure 4(b), LDPE minor-component film layers ranged from 15 to $90 \mu\text{m}$. The intervening major component PS layers are thicker in accordance with the blend composition (6.4% by volume).

Although the starting point was a simple rod located as shown in Figure 2, further chaotic mixing acted on the more complex shape in Figure 4(a) to give a rapid increase in the number of film layers and decrease in layer thicknesses. Compositional uniformity was also attained over increasingly larger regions and at smaller scales by virtue of mutual phase envelopment and refinement that are characteristic of chaotic mixing. For $N \geq 4$, optical microscopy was insufficient to resolve the films produced. Freeze-fractured sur-



(a)



(b)

Figure 5 Freeze-fractured samples for (a) $N = 4$, with multilayers of PS and LDPE, and (b) $N = 8$, containing more and thinner PS and LDPE layers.

faces in the region of the narrow gap between the inner and outer cylinders were therefore examined by low-voltage SEM. To clearly expose the films, surfaces were exposed mainly perpendicular to the cavity cylinder axes. Typical microstructures for $N = 4$ are shown in Figure 5(a). Thin LDPE films were present between thicker PS films and the films were oriented along the flow direction indicated by superimposed arrows. Because of poor adhesion between PS and LDPE, some films separated upon fracture, exposing continuous unbroken layers. In Figure 5(b), thinner film layers are apparent that corresponded to a longer processing time ($N = 8$). Delamination did not occur among the thinner layers in contrast to Figure 5(a). Comparisons between Figure 5(a) and 5(b) also demonstrate that film-layer thick-

ness can be readily controlled in related continuous flow processes such as the one depicted in Figure 1.

A high-magnification view of the layers in Figure 5(b) are given in Figure 6. Thinner LDPE layers are intermingled with thicker PS layers with relative thicknesses reflecting the 6.4% LDPE volume concentration. The thinnest layers have thicknesses of less than $2 \mu\text{m}$. It should be noted that much finer film layers can be produced in polymer combinations having lower interfacial tension. For example, interfacial tension for the much finer PP/EPDM films of Figure 1(a) was about 1.1 dyn/cm^5 in comparison to the higher interfacial tension of 4.5 dyn/cm for the films in Figure 6. Unlike coextrusion, it is evident that extruded multilayer films produced by chaotic mixing will contain layers of different thicknesses even for the same polymer component. Differences in layer thicknesses arise because of spatially nonuniform stretching and folding rates that are characteristic of chaotic mixing conditions, as discussed earlier. These differences can be made smaller by careful design and operation of chaotic mixing devices.

To elucidate subsequent morphology development, 2- to 5-mm-thin disk sections were cut from whole samples produced for a specific number of mixing periods within the range $10 \leq N \leq 23$. These sections were immersed in toluene to extract the PS matrix. The undissolved LDPE was isolated by using filter paper. In Figure 7, broken LDPE film layers that were liberated from the PS are shown for $N = 10$. The layers were taken from the large gap between the inner and outer cylinders (Fig. 2). Close inspection revealed that individual layers were interconnected. The sample had a spongy response to mechanical deformation in contrast to samples containing disconnected films similarly liberated by dissolution. Because the PS phase had occupied the irregularly shaped holes prior to dissolution and the liberated broken LDPE layers were interconnected, it can be concluded that the multilayer film morphologies of Figures 5 and 6 were converted upon additional chaotic mixing to an interpenetrating blend. The transition from a multilayer film to an interpenetrating blend may have occurred because of simultaneous instabilities in both the LDPE and the PS layers. For example, in Figure 6, simultaneous hole formation in the LDPE and PS layers would lead to an abrupt conversion of the blend morphology. (This morphology transition is discussed further below.) Interpenetrating blends of

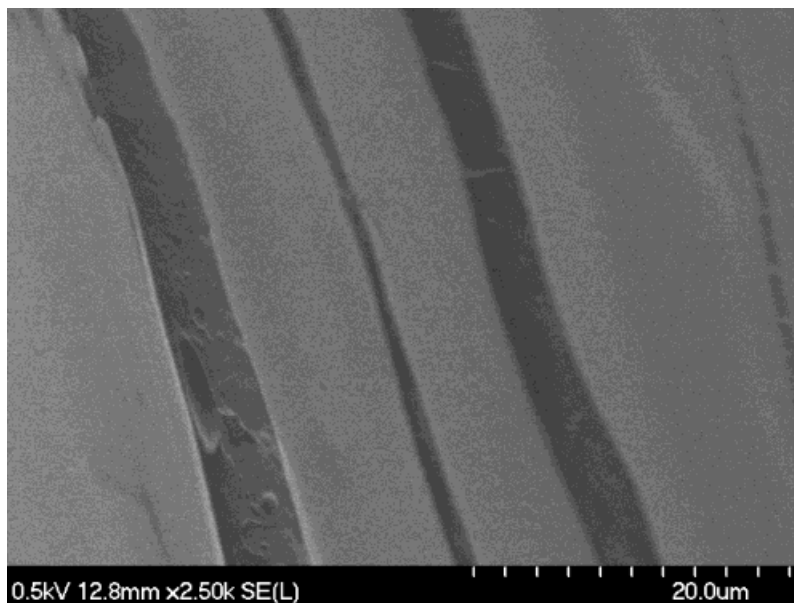


Figure 6 Thin LDPE layers in a freeze-fractured sample ranging in thickness from 1 to 4 μm for $N = 8$.

the type shown in Figure 7 are made possible by progressively forming and refining multilayer films. It is noteworthy that they were formed at a very low 6.4% LDPE volume composition, whereas more intermediate compositions are specified by common blending formulae.²² Regions also existed at other points within the sample where films remained intact owing to the aforementioned differences in rates of morphology development that occurred. These spatial differences were characteristic of the chaotic mixing cavity of Figure 2 and can be less significant in other chaotic mixing devices that generate more spatially uniform stretching and folding rates over time. Good uniformity was obtained, for example, in the extruded films shown in Figure 1 by using a chaotic mixer with two internal stir rods.⁵

In contrast to the interpenetrating blend of Figure 7, parallel disconnected LDPE and PS films were also found in the mixing cavity with unbroken lengths of about 10 cm and thicknesses ranging from 5 to 50 μm . LDPE films for $N = 23$ in Figure 8 had holes with diameters of about 200 μm . Because the layers were disconnected, it can be surmised that holes had not formed in the thicker PS films that had been removed by dissolution. The morphology thereby had a useful single phase continuity within the PS component that would greatly reduce delamination. Fewer and smaller 20- μm holes were found in samples processed for shorter times ($N = 10$). The holes grew in size and number as chaotic mixing pro-

ceeded and were aligned predominantly in the melt-flow direction indicated by the overlaid arrow in the low-magnification view in Figure 8. Droplets were also collected during dissolution. Some were deposited on the liberated films and can be seen in the high-magnification view. The droplet sizes of 1–10 μm were comparable to the film thicknesses because they were derived from film breakup. The presence of droplets with diameters similar to the film thicknesses and the ab-

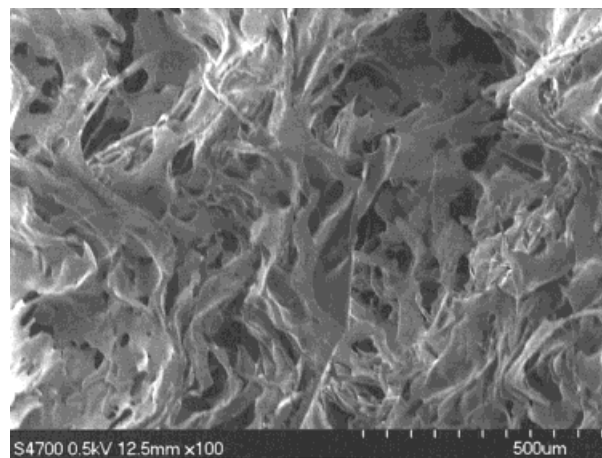


Figure 7 SEM micrographs of interconnected LDPE structures liberated by dissolution and viewed in the x - y plane (Fig. 2) for $N = 10$. Because the removed PS phase was continuous, an interpenetrating blend was formed.

sense of elongated shapes such as fibers elucidated film breakup mechanisms. Sferrazza et al.²³ and Yerushalmi-Rozen et al.²⁴ showed that liquid films on liquid substrates can break up by an interfacially driven dewetting process in which holes form and coalesce to directly yield droplets. Hole formation in this spinodal dewetting process occurred more quickly in films having higher interfacial tension and smaller thickness and in the absence of impurities that can serve as hole nucleation sites. Studies such as these with single-film layers on deformable liquid substrates provide insights about how holes may form in the multilayer films of this study. However, hole formation and film breakup were more complex because of layer interactions and simultaneous refinement processes that continued to act on the layers (Fig. 1).

For $60 \leq N \leq 100$, film breakup was complete and a structured distribution of very fine droplets

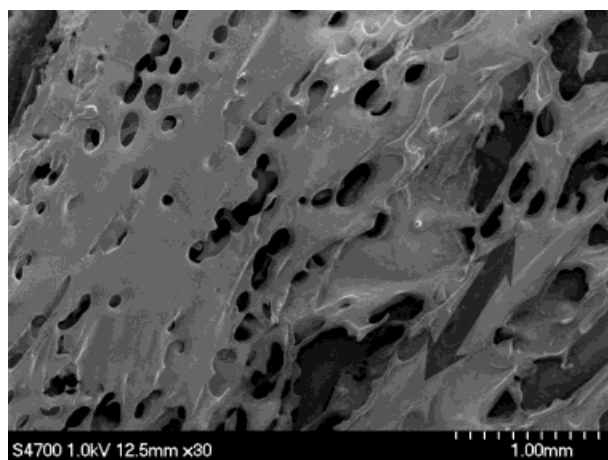


Figure 8 Low- and high-magnification SEM micrographs of liberated LDPE films collected near the inner cylinder for $N = 23$.

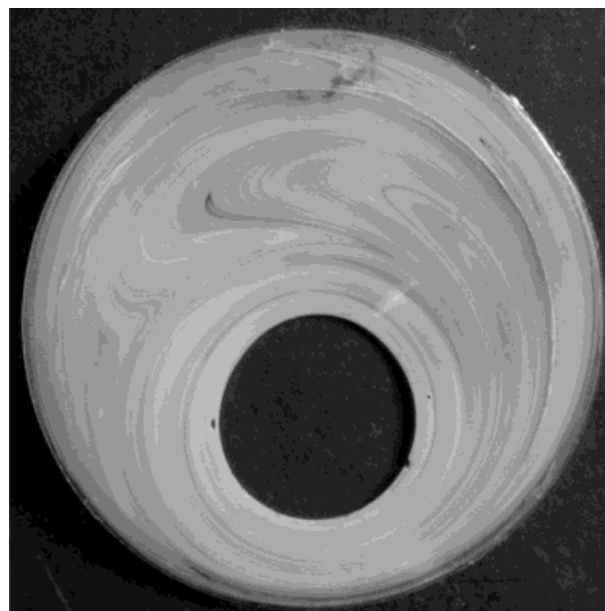


Figure 9 Patterns formed among droplets after complete film breakup ($N = 80$) in a 300- μm -thick section.

with sizes ranging from 1 to 10 μm resulted. Many droplets tended to be aligned because they were derived from multilayer film breakup. In Figure 9, patterns among droplets are evident within a thin microtomed cross section that were reminiscent of the parent film layers. Interestingly, the early film layers of Figure 4 were converted progressively with additional processing to the multilayer films of Figures 5 and 6, to the novel interconnected morphologies of Figures 7 and 8, and finally to a distribution of droplets retaining features of the parent film layers. The structured droplet distribution differed from the random droplet dispersions normally obtained by conventional blending techniques for this polymer system.

In Figure 10, the dimensions of sheets ($>200 \mu\text{m}$ thick), films, and droplets are summarized in terms of the elapsed processing time represented by the N number of mixing periods. Dimensions correspond to the average size of PS structures, whereas range bars indicate the minimum and maximum dimensions that were present. The initial LDPE minor component in rod form and the surrounding PS (Fig. 2) were rapidly converted *in situ* to sheets and multilayer films by recursive stretching and folding that characterizes chaotic mixing. Films were created in both components as each became folded about the other and stretched by shear deformation. The rate of reduction in layer thickness slowed as surrounding PS became

incorporated into the multilayer blend and because of viscosity differences and interfacial tension known to slow shear-induced deformations.^{6,7} After refinement to below about 20 μm , blends with single- and dual-phase continuity were formed in concert with droplets. Film layers and their interconnections eventually subdivided to yield oriented droplets. The droplet diameters ranged from 1 to 10 μm and remained unchanged even after long processing times (e.g., $N = 100$). This range in droplet sizes was determined to be in excellent agreement with Taylor's expression for droplet deformation for the range of shear rates existing within the mixing cavity.²⁵ However, the agreement may be coincidental in that droplet diameters were also consistent with the film-layer thicknesses, as described earlier. The multilayer film breakup suggests opportunities to create droplets with very small diameters. Such droplets would coalesce and break up over time to yield dispersions consistent with Taylor's expression. The relation of droplet diameter to parent film-layer thickness is a subject of ongoing work.

The progressive morphology development and key morphology transitions are summarized in Figure 11. The relative abundance of each shape changed with elapsed processing time. The initially large minor component rod was quickly transformed into localized sheets that refined to become multilayer films. The LDPE films were generally thinner than the PS films because of a smaller volume fraction and because the PS more readily deformed the less viscous LDPE compo-

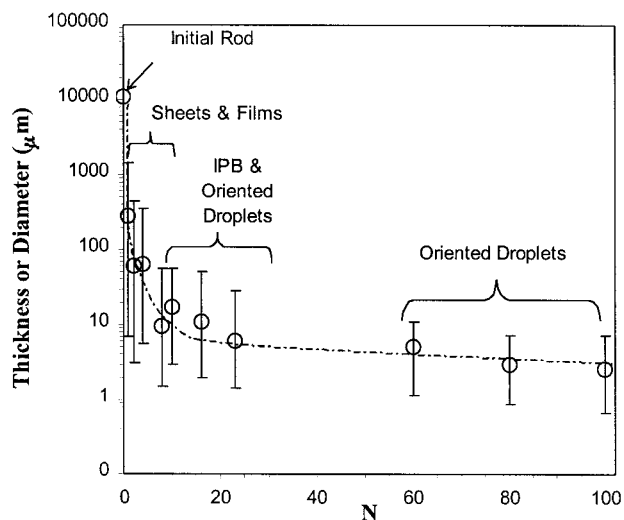


Figure 10 Layer thickness, droplet sizes, and blend morphologies obtained in terms of the number N of mixing periods. (Range bars represent maximum and minimum sizes of LDPE structures.)

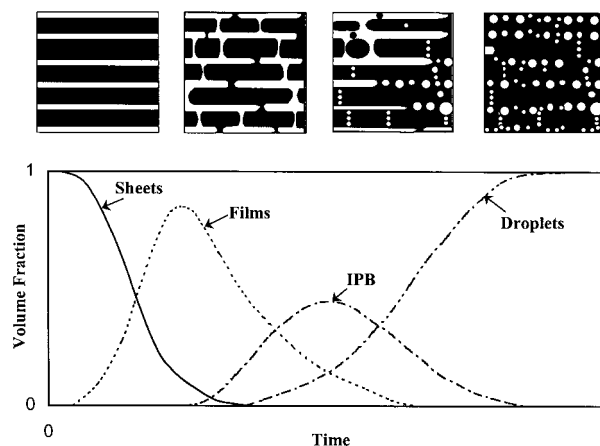


Figure 11 Qualitative summary of the progressive formation of specific blend morphologies and morphologic transitions.

nent. After refinement below 1 to 10 μm , holes developed in the LDPE films. Hole development resulted in the formation of interconnections between adjacent PS layers and the abrupt conversion of the multilayer morphology to a blend with single-phase continuity in the PS component. After further layer refinement, additional holes formed in the LDPE layers and holes also formed in the thicker PS layers. The LDPE layers became similarly interconnected to yield a blend with dual phase continuity (i.e., an interpenetrating blend). Hole sizes increased with increasing N . Hole formation was accompanied by LDPE droplet formation because the holes through the thicker intervening PS layers constituted thin threads which broke via capillary instabilities. A distribution of oriented LDPE droplets was finally obtained within PS where the droplet positions reflected the locations of parent film layers from which they were formed. Some LDPE droplets appeared between the parent LDPE film layers having been formed from the breakup of interconnecting thin threads (i.e., holes) between film layers. It should be noted that all of the morphologies in Figures 4–9 were obtainable at the single 6.4% by volume composition. The degree of morphology development during chaotic mixing was readily controlled by mixing time or by selection of other parameters related to the chaotic mixing condition, such as the rotational displacement of the cylinders in Figure 2. Extrusions with uniform multilayer film morphologies, film layers of desired thicknesses, and film layers with different extents of breakup have been produced by changing the number of mixing periods in related continuous flow devices, for example.^{5,10}

CONCLUSION

Extrusions with multilayer film morphologies have been produced by a chaotic mixing process with layer thicknesses below 200 nm in some polymer combinations. To facilitate morphology inspections by obtaining larger film thicknesses and breakup bodies, LDPE as the minor component and PS were selected in this study and a related batch process was employed. Long and unbroken LDPE films developed quickly and became distributed throughout the cavity volume. The PS major component was similarly converted into film form as both the LDPE and the PS were stretched and folded about one another. Film thicknesses decreased rapidly with processing time and a multilayer morphology arose throughout the cavity volume. After refinement, holes developed in the LDPE films to abruptly convert the multilayer morphology to a blend with single-phase continuity. After further layer refinement, additional holes formed in the LDPE layers and holes also formed in the thicker PS layers. The LDPE layers also became interconnected to yield a blend with dual-phase continuity (i.e., an interpenetrating blend). Hole formation was accompanied by LDPE droplet formation because the holes through the thicker intervening PS layers constituted thin threads which broke via capillary instabilities. A distribution of oriented LDPE droplets was finally obtained within the PS where the droplet positions reflected the locations of parent film layers from which they were formed. Although the multilayer film morphologies are desirable for many applications, it is also suggested by these results that other useful blend morphologies might be obtainable with an improved understanding of multilayer film breakup, such as blends with single- or dual-phase continuity over broad compositional ranges, multilayer films containing holes of desired sizes, blends with platelet morphologies, and droplets with diameters similar to the thicknesses of parent film layers. Blends with single- and dual-phase continuity and also a predominant multilayer morphology can provide the means to reduce layer delamination in extruded films. Chaotic mixing also offers opportunities to progressively and controllably form fine-scale structures in melts via simple motions of bounding surfaces and may serve as a basis for automated blending devices. For example, changes to morphology can be made on-line to give desired properties in extrusions.^{5,10}

Financial support was provided by the Engineering Research Center Program of the National Science Foundation under Award No. EEC-9731680 and by the 3M Company.

REFERENCES

1. Finch, C. R.; in *Multilayer Films*; T. Kanai; G. A. Campbell, Eds.; Film Processing; Hanser Publishers: Cincinnati, 1999; pp 228–241.
2. Im, J.; Baer, E.; Hiltner, A.; in *Microlayer Composites*; E. Baer; A. Moet, Eds.; High Performance Polymers; Hanser Publishers: Cincinnati, 1991; pp 175–198.
3. Ma, M.; Vijayan, K.; Hiltner, A.; Baer, E. *J Mater Sci* 1990, 25, 2039–2046.
4. Lee, S. Y.; Kim, S. C. *Polym Eng Sci* 1997, 37, 463.
5. Zumbunnen, D. A.; Inamdar, S. *Chem Eng Sci* 2001, 56, 3893–3897.
6. Harnby, N.; Edwards, M. F.; Nienow, A. W. *Mixing in the Process Industries*, 2nd ed.; Butterworth-Heinemann: Oxford, 1997; p 200–208.
7. Zhang, D.; Zumbunnen, D. A. *J Fluids Eng* 1996, 118, 40.
8. Liu, Y. H.; Zumbunnen, D. A. *Polym Composites* 1996, 17, 187.
9. Liu, Y. H.; Zumbunnen, D. A. *J Mater Sci* 1999, 34, 1921–1931.
10. Zumbunnen, D. A. *J Textile Inst (Part 3)* 2000, 91, 92–104.
11. David, C.; Trojan, M. *Polymer* 1991, 32, 510–515.
12. David C.; Getclichermann, M.; Trojan, M. *Polym Eng Sci* 1992, 32, 6–13.
13. Subramanian, P. M.; Mehra, V. *Polym Eng Sci* 1987, 27, 663–668.
14. Zumbunnen, D. A.; Miles, K. C.; Liu, Y. H. *Composites Part A* 1996, 27, 37–47.
15. Aref, H.; Balachandar, S. *Phys Fluids* 1986, 29, 3515–3521.
16. Swanson, P. D.; Ottino, J. M. *J Fluid Mech* 1990, 213, 227–240.
17. Liu, M.; Muzzio, F. J.; Peskin, R. L. *Chaos, Solitons Fractals* 1994, 4, 869–893.
18. Stone, H. A.; Leal, L. G. *J Fluid Mech* 1989, 198, 399–427.
19. Zhang, D.; Zumbunnen, D. A. *AIChE J* 1998, 44, 442–451.
20. Sanchez, I. C. *Polym Eng Sci* 1984, 24, 79–85.
21. Willemsse, R. C.; Boer, A. P.; van Dam, J.; Gotsis, A. D. *Polymer* 1998, 39, 5879–5887.
22. Paul, D. R.; Barlow, J. W. *J Macromol Sci, Rev Macromol Chem* 1980, C18, 109–168.
23. Sferazza, M.; Heppenstall-Butler, M.; Cubitt, R.; Bucknall, D.; Webster, J.; Jones, R. A. L. *Phys Rev Lett* 1998, 81, 5173–5176.
24. Yerushalmi-Rozen R.; Kerle, T.; Klein, J. *Science* 1999, 285, 1254–1256.
25. Taylor, G. I. *Proc R Soc London* 1934, A146, 501–523.